J Mol Model (2011) 17:3173–3181
DOI 10.1007/s00894-011-0979-6

ORIGINAL PAPER

Theoretical mechanistic study of the reaction of the methylidyne radical with methylacetylene

Lili Zhang · Hui-ling Liu · Guang-Hui Yang · Xu-ri Huang · Yan Li · Yan-bo Sun · Chia-chung Sun

Received: 24 November 2010 / Accepted: 18 January 2011 / Published online: 2 March 2011

Abstract A detailed doublet potential energy surface for the reaction of CH with CH_3CCH is investigated at the B3LYP/6-311G(d,p) and G3B3 (single-point) levels. Various possible reaction pathways are probed. It is shown that the reaction is initiated by the addition of CH to the terminal C atom of CH_3CCH, forming CH_3CCHCH **1** (**1a**,**1b**). Starting from **1** (**1a**,**1b**), the most feasible pathway is the ring closure of **1a** to CH_3–cCCHCH **2** followed by dissociation to $\mathbf{P_3}$(CH_3–cCCCH+H), or a 2,3 H shift in **1a** to form CH_3CHCCH **3** followed by C–H bond cleavage to form $\mathbf{P_5}$(CH_2CHCCH+H), or a 1,2 H-shift in **1** (**1a**, **1b**) to form CH_3CCCH_2 **4** followed by C–H bond fission to form $\mathbf{P_6}$(CH_2CCCH_2+H). Much less competitively, **1** (**1a**,**1b**) can undergo 3,4 H shift to form $CH_2CHCHCH$ **5**. Subsequently, **5** can undergo either C–H bond cleavage to form $\mathbf{P_5}$ (CH_2CHCCH+H) or C–C bond cleavage to generate $\mathbf{P_7}$ (C_2H_2+C_2H_3). Our calculated results may represent the first mechanistic study of the CH + CH_3CCH reaction, and may thus lead to a deeper understanding of the title reaction.

Keywords Density functional calculations · Carbenes · Radical reaction · Reaction mechanism

L. Zhang · H.-l. Liu · X.-r. Huang (✉) · Y. Li · Y.-b. Sun · C.-c. Sun
State Key Laboratory of Theoretical and Computational Chemistry, Institute of Theoretical Chemistry, Jilin University, Changchun 130023, People's Republic of China
e-mail: xurihuang@gmail.com

L. Zhang
e-mail: lilizhang2010fly@gmail.com

G.-H. Yang
JiLin Provincial Institute of Education, Changchun 130022, People's Republic of China

Introduction

The methylidyne radical (CH) is a very reactive species as the C atom contains one singly occupied orbital and one vacant nonbonding orbital. It plays very important roles in combustion, atmospheric, and interstellar chemistry [1–6]. Up to now, a large number of experimental and theoretical studies have been carried out on the spectroscopic properties of CH [7–12] and its reactions [13–26] such as those with O_2, N_2, CH, NH_3, H_2S, CH_4, C_2H_6, C_3H_8, C_4H_{10}, C_5H_{12}, C_2H_4, C_3H_6, C_4H_8, C_2H_2, CH_3CCH, and so forth.

Among the numerous studies that have been made of the CH radical, its reaction with CH_3CCH is the one that has most attracted the authors' interest. The reaction mechanism is still unclear, although it has been experimentally studied by several groups. In 2005, Daugey et al. [21] investigated the reaction using a supersonic flow reactor coupled with the pulsed laser photolysis (PLP) and laser-induced fluorescence (LTF) techniques. The total rate constant was reported for the first time in that study. The measured rate constant over the temperature range 15–295K was $k = (4.03 \sim 4.56)\times 10^{-10} cm^3 molecule^{-1} s^{-1}$. Daugey et al. also proposed that the reaction is initiated by the attachment of the CH radical to the terminal carbon atom of CH_3CCH, forming a chainlike intermediate. The intermediate can then undergo various evolution pathways, leading to the final products. They also suggested that 1,2,3-butatriene and hydrogen were the main products. In 2008, Loison et al. [25] studied the same reaction in a low-pressure fast-flow reactor at room temperature and proposed similar mechanisms. The rate constant obtained by Loison et al. was $k(300K) = (3.4 \pm 0.6) \times 10^{-10} cm^3 molecule^{-1} s^{-1}$. In the same year, Goulay et al. [26] investigated the reaction using tunable vacuum ultraviolet (VUV) photoionization and time-resolved mass spectrometry. In that report, three channels leading to the cyclic isomer + H (30%), vinylacetylene + H (37%), and 1,2,3-butatriene + H (33%) were proposed. Obviously, Goulay et al.'s results differ significantly from those obtained by Daugey et al. [21] and Loison et al. [25].

In view of the potential importance and significant discrepancies between the results of those studies, a detailed potential energy surface (PES) study of the title reaction is very desirable. Unfortunately, no such theoretical study has been reported, to the best of our knowledge. Therefore, we performed a detailed theoretical study on the reaction of CH with CH_3CCH to explore the reaction mechanism, and the results of that study are reported here.

Computational methods

All the calculations were carried out using the Gaussian 03 software package [27]. The optimized structures and frequencies of all species, including reactant, products, isomers, and transition states, were obtained at the B3LYP/

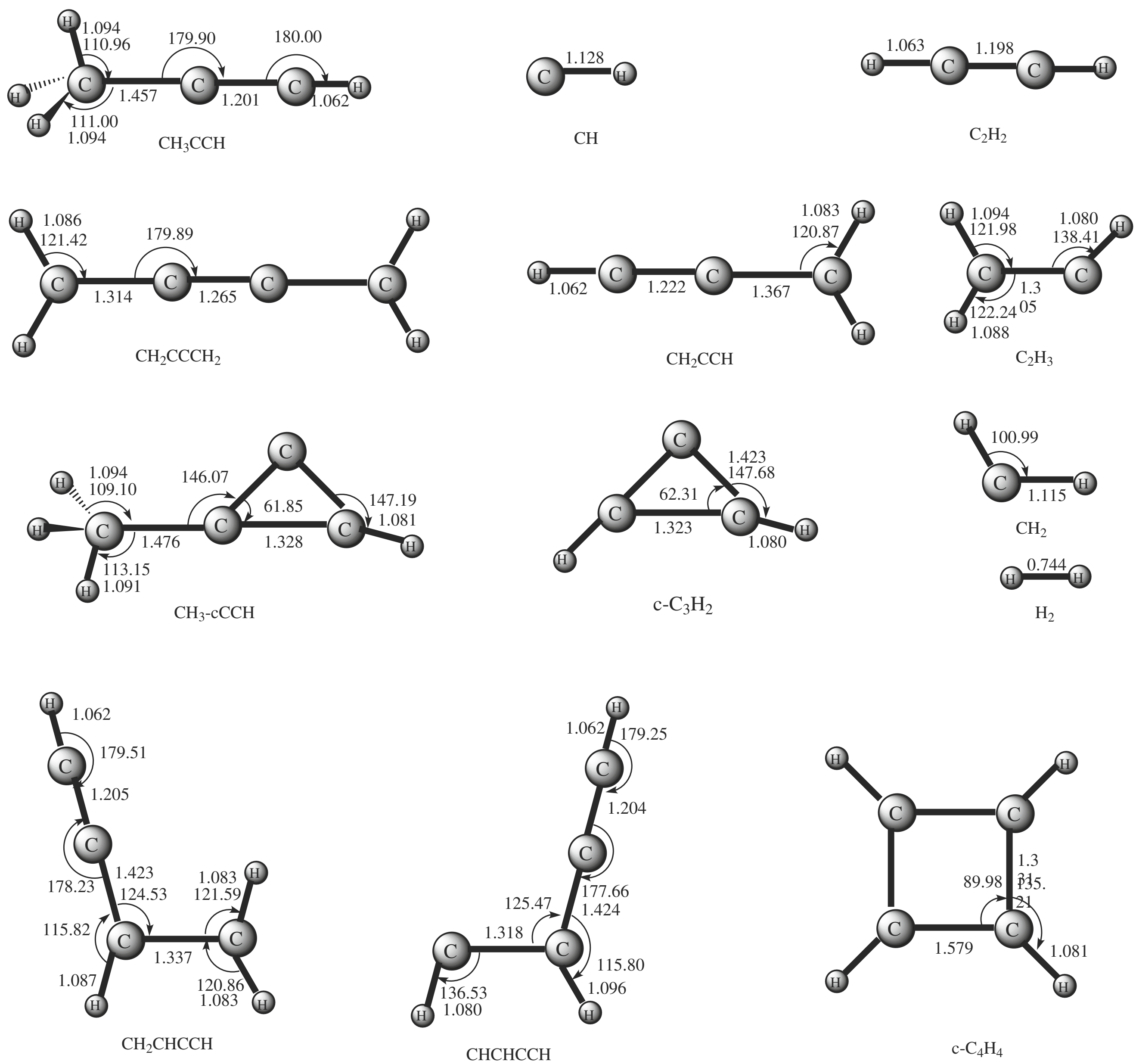

Fig. 1 The optimized structures of the reactant and products at the B3LYP/6-311G(d,p) level. Distances are given in angstroms and angles in degrees

6-311G(d,p) level. Single-point energy calculations were performed at the G3B3 level using the B3LYP/6-311G(d, p)-optimized geometries and were scaled by the B3LYP/6-311G(d,p) zero-point energies. To confirm that the transition states were associated with the designated isomers, intrinsic reaction coordinate (IRC) calculations were performed at the B3LYP/6-311G(d,p) level.

Results and discussion

The optimized structures of the reactant and products are shown in Fig. 1, while the optimized structures of isomers and transition states are shown in Figs. 2 and 3, respectively. The schematic potential energy surface (PES) of the CH+CH_3CCH reaction at the G3B3//B3LYP/6-311G (d,p) level is plotted in Fig. 4, and Fig. 5 shows the dissociation curves to the products. The energetic data for the reactant, products, isomers, and transition states are listed in Table 1. The total energy of the reactant CH+CH_3CCH was set to zero for reference. Unless otherwise specified, the G3B3//B3LYP/6-311G(d,p) relative energies are used throughout.

Entrance channels

The CH radical can attach to the CH_3CCH molecule in three ways: (i) to the terminal C atom to form CH_3CCHCH **1** (**1a**, **1b**) (−29.7, 32.7); (ii) the CH carbene inserts itself into the C–H σ-bond of the –CH_3 radical to generate CH_2CH_2CHCH **8** (−94.2), or; (iii) H abstraction to form $\mathbf{P_1}$ (CH_2CCH+CH_2) (−0.4). Values in parentheses are the G3B3//B3LYP/6-311G (d,p) relative energies in kcal mol^{-1} with reference to **R** (CH+CH_3CCH) (0.0). Channels (ii) and (iii), with their high-energy transition states **TS8/11** (18.0) and $\mathbf{TS11/P_1}$ (19.9), are of no practical interest. Thus, only the formation of **1** appears possible, a conclusion that is supported by orbital analysis. At the B3LYP/6-311G(d,p) level, the HOMO and LUMO

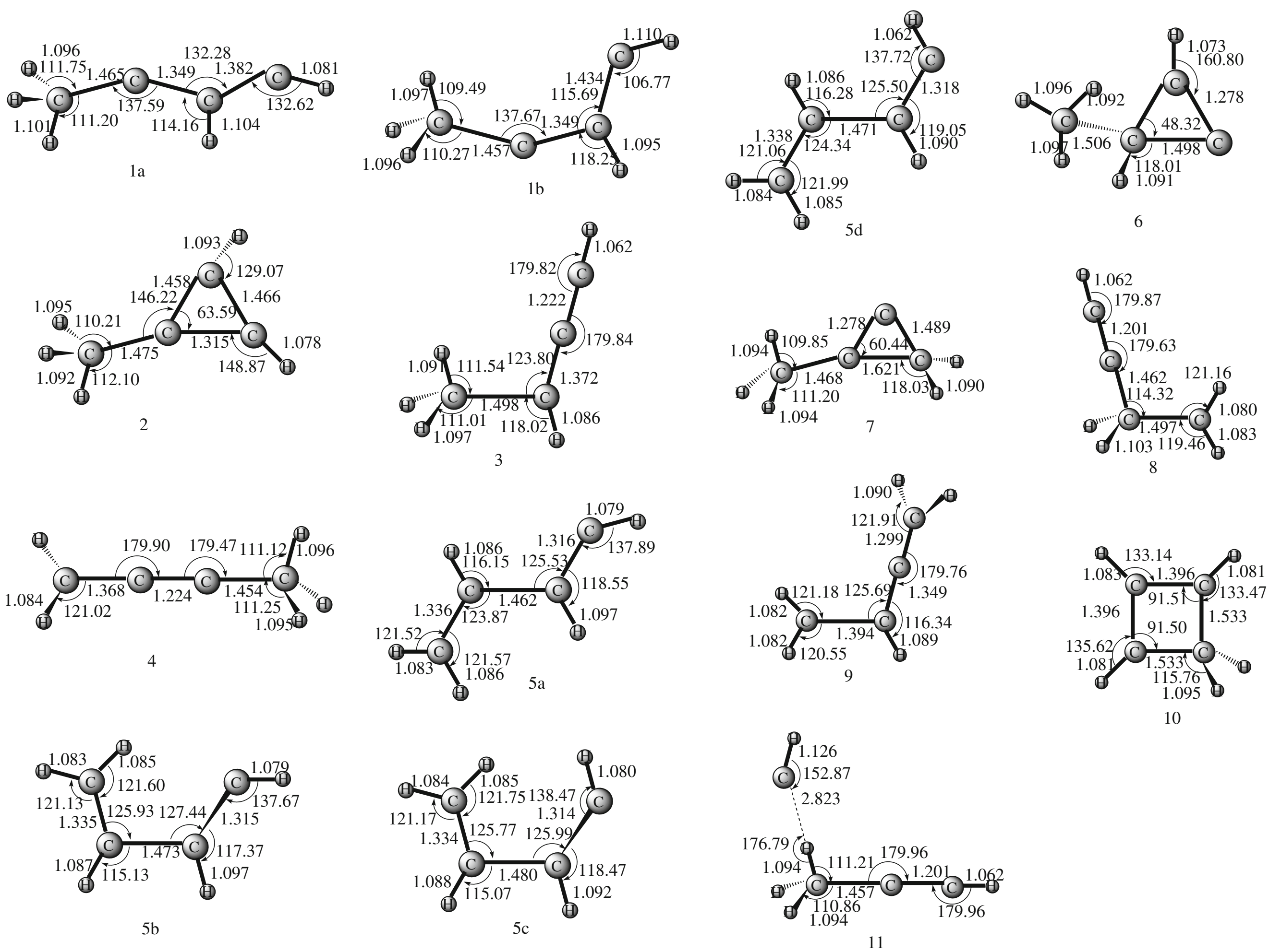

Fig. 2 The optimized structures of the isomers at the B3LYP/6-311G(d,p) level. Distances are given in angstroms and angles in degrees

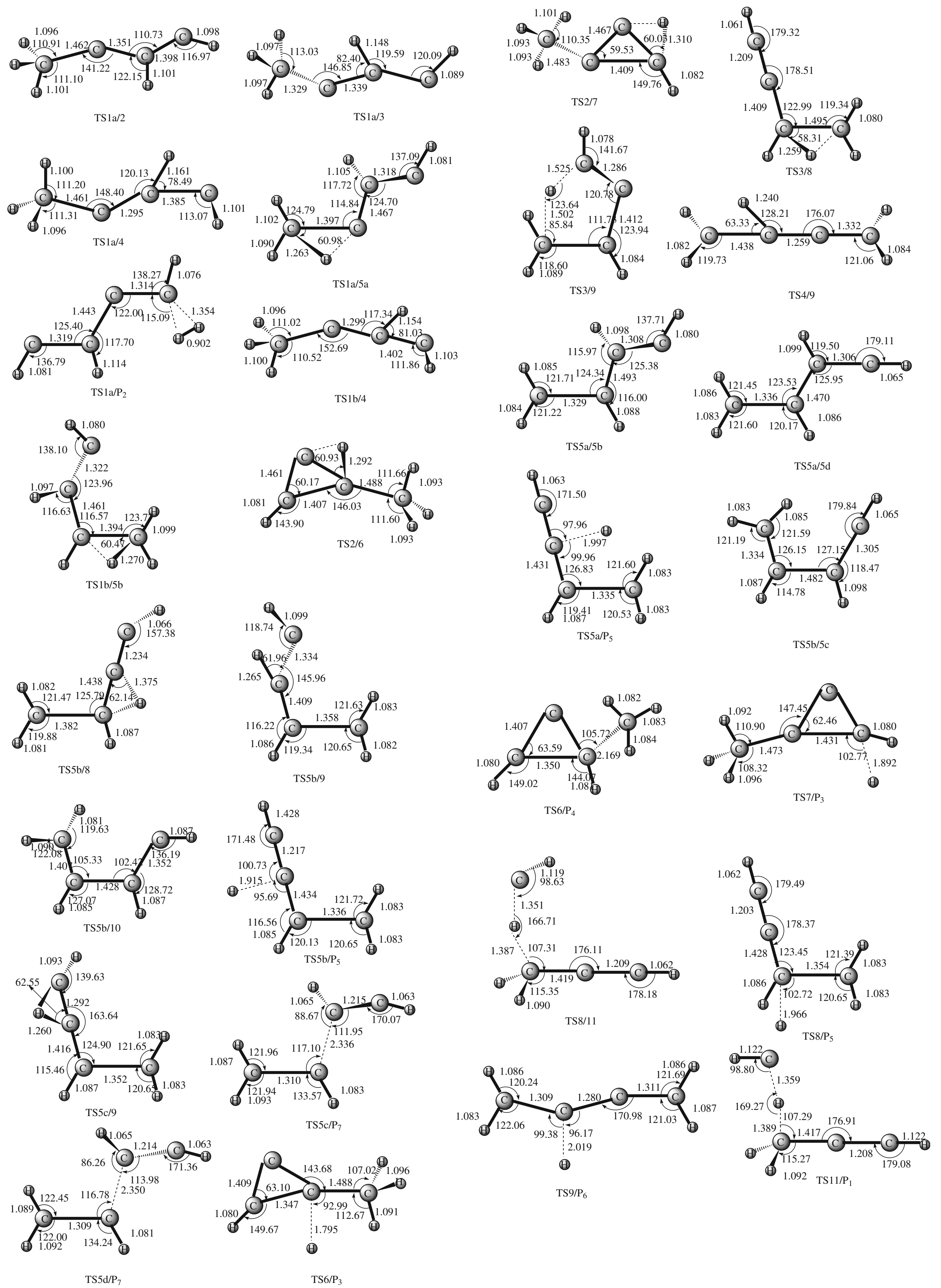

TS1a/2
TS1a/3
TS2/7
TS3/8
TS1a/4
TS1a/5a
TS3/9
TS4/9
TS1a/P_2
TS1b/4
TS5a/5b
TS5a/5d
TS1b/5b
TS2/6
TS5a/P_5
TS5b/5c
TS5b/8
TS5b/9
TS6/P_4
TS7/P_3
TS5b/10
TS5b/P_5
TS8/11
TS8/P_5
TS5c/9
TS5c/P_7
TS9/P_6
TS11/P_1
TS5d/P_7
TS6/P_3

◀**Fig. 3** The optimized structures of the transition states at the B3LYP/6-311G(d,p) level. Distances are given in angstroms and angles in degrees

energies of CH are −0.25590 and −0.12643 a.u., respectively, while those of CH_3CCH are −0.27174 and 0.04683 a.u., respectively. The absolute energy difference between E($HOMO_{CH3CCH}$) and E($LUMO_{CH}$), 014531, is smaller than the difference of 0.30273 a.u. between E($HOMO_{CH}$) and E($LUMO_{CH3CCH}$). Based on frontier orbital rules, the interaction should take place between the LUMO of CH and the HOMO of CH_3CCH, resulting in the addition intermediate **1**. In the following section, we will mainly discuss the evolution pathways of **1**.

Isomerization and dissociation

The most important pathways from **1a** are shown in a concise manner in Scheme 1.

This scheme shows that, starting from CH_3CCHCH **1a** (−29.7), five conversion channels can be identified: (i) direct ring closure to form CH_3–cCCHCH **2** (−78.8); (ii) a 2,3 H shift to form CH_3CHCCH **3** (−107.9); (iii) a 1,2 H shift to form CH_3CCCH_2 **4** (−110.8); (iv) a 3,4 H shift to form $CH_2CHCHCH$ **5a** (−96.9), or; (v) H_2 elimination to form $\mathbf{P_2}$ ($CHCHCCH+H_2$) (−56.0). Channel (v) is unfeasible, since its transition state **TS1a/P$_2$** (6.5) is higher than the reactant in energy.

Starting from the isomer CH_3–cCCHCH **2**, three kinds of pathways can be identified: (i) H elimination to form $\mathbf{P_3}$ (CH_3–cCCCH+H) (−28.2); (ii) an H shift along the ring to form CH_3–cCHCCH **6** (−67.7), which can undergo H or CH_3 elimination to generate $\mathbf{P_3}$ (CH_3–cCCCH+H) or $\mathbf{P_4}$ (c–C_2H_3+CH_3) (−32.1), respectively, or; (iii) isomerization to CH_3–cCCCH$_2$ **7** (−70.2) followed by H elimination to form $\mathbf{P_3}$(CH_3–cCCCH+H). It should be noted that the conversion **2**→$\mathbf{P_3}$ in channel (i)

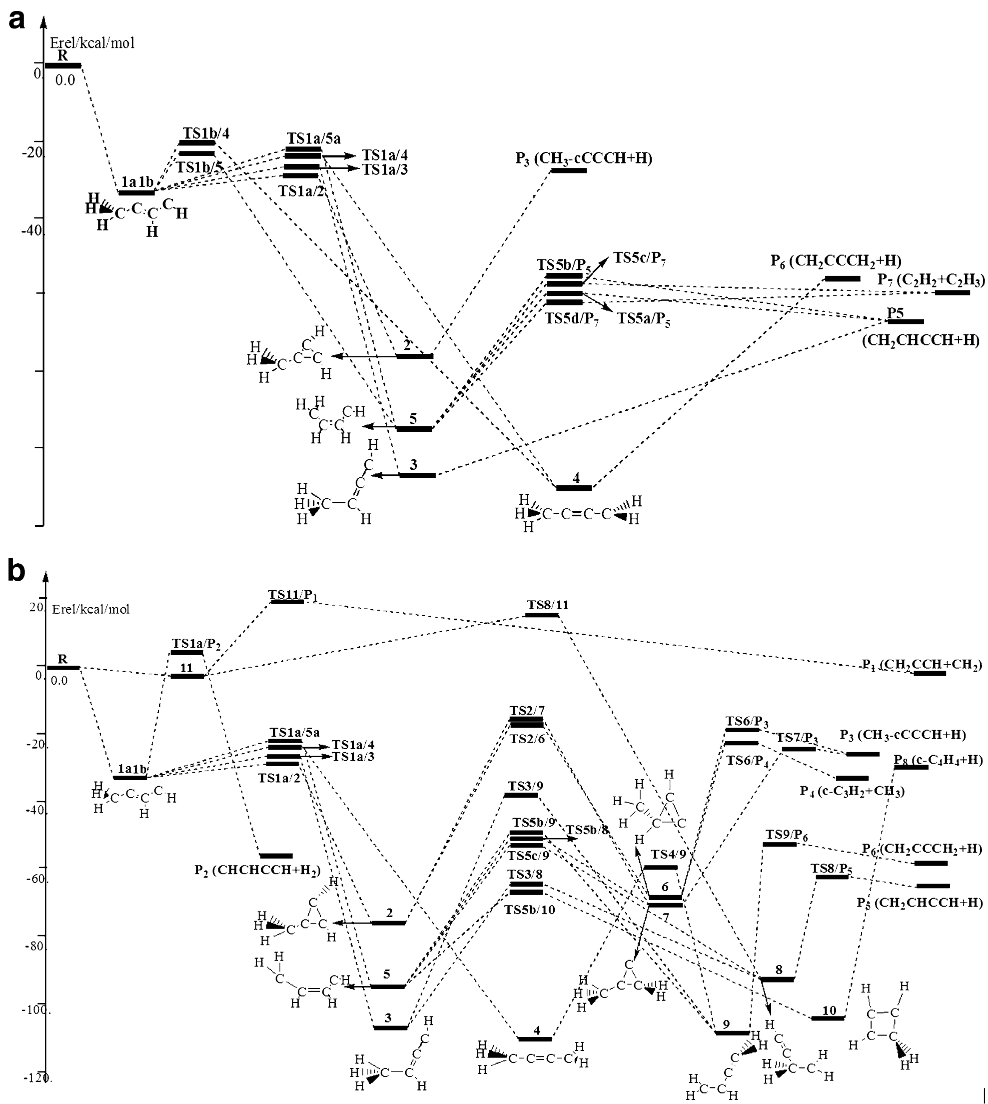

Fig. 4 a–b Pathways for the $CH+CH_3CCH$ reaction. *Erel* is the relative energy (kcal mol^{-1}). Competitive pathways are shown in **a** and less competitive pathways in **b**

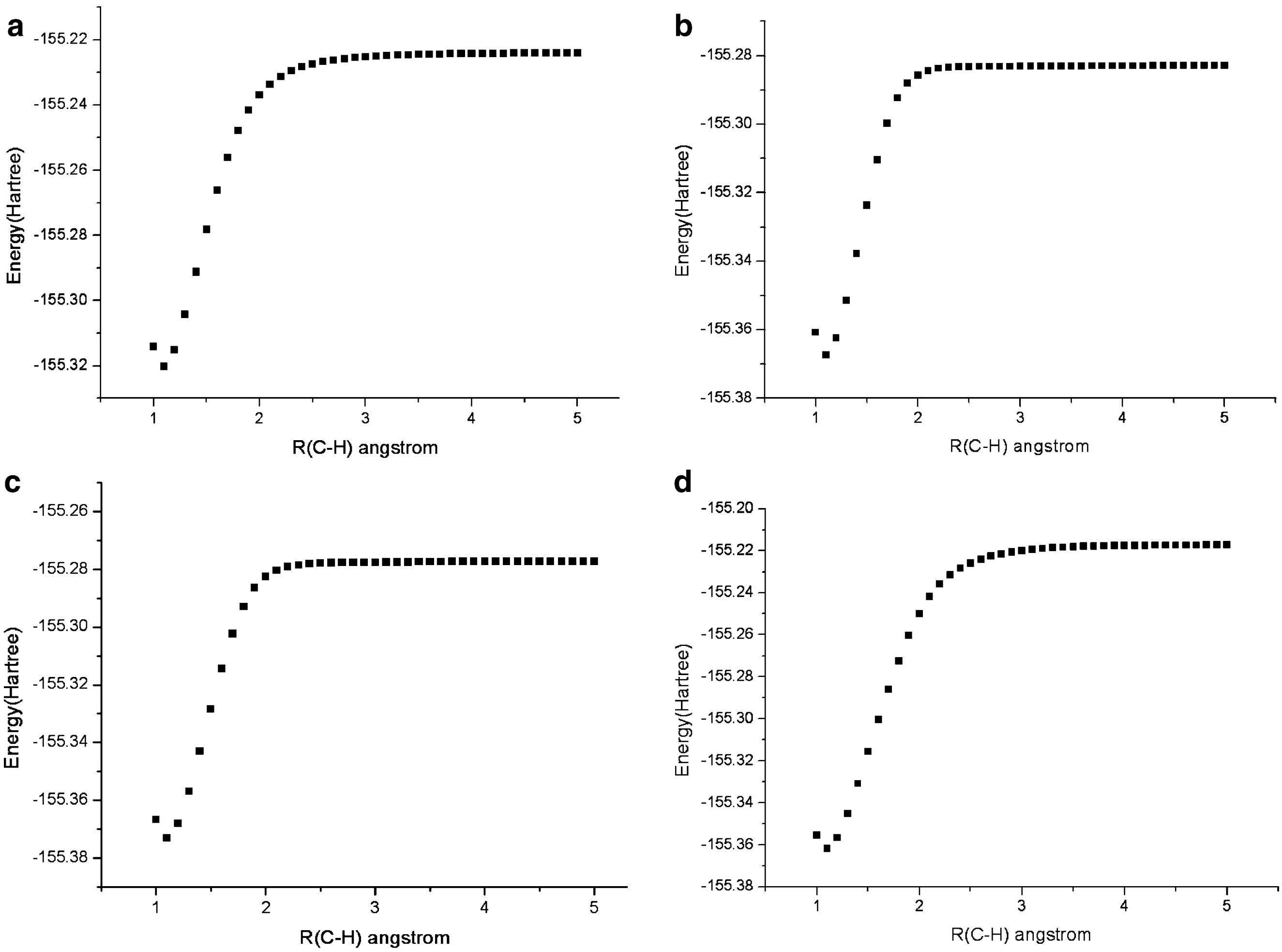

Fig. 5a–d Dissociation curves computed at the B3LYP/6-311G(d,p) level for **2**→$\mathbf{P_3}$; **3**→$\mathbf{P_5}$; **4**→$\mathbf{P_6}$; and **10**→$\mathbf{P_8}$ (shown in **a**–**d**, respectively)

is a barrierless process, as confirmed by the pointwise potential energy curve at the B3LYP/6-311G(d,p) level, while high-energy barriers need to be surmounted in the latter two channels. Thus, channel (i) may be virtually the only process from **2**.

For the isomer CH_3CHCCH **3**, three channels can be discerned : (i) a 1,2 H shift to form CH_2CH_2CCH **8** (−94.2), followed by dissociation to $\mathbf{P_5}$ (CH_2CHCCH+H) (−65.1); (ii) a 1,4 H shift to form CH_2CHCCH **9** (−108.5), followed by dissociation to $\mathbf{P_6}$ (CH_2CCCH_2+H) (−57.8), or; (iii) direct dissociation to $\mathbf{P_5}$ (CH_2CHCCH+H). To further confirm that channel (iii) is a barrierless process, we calculated the pointwise potential curve at the B3LYP/6-311G(d,p) level. The dissociation curve of **3** is shown in Fig. 5b. Since higher barriers need to be surmounted in channels (i) and (ii), these two channels can be neglected.

The isomer CH_3CCCH_2 **4** can directly dissociate to $\mathbf{P_6}$ (CH_2CCCH_2+H) (−57.8) without the need to cross any barrier. The dissociation curve of **4** is shown in Fig. 5c. Alternatively, **4** can undergo a 1,2 H shift and then H elimination to form CH_2CHCCH_2 **9** (−108.5) and then $\mathbf{P_6}$ (CH_2CCCH_2+H). The latter process is undoubtedly much less kinetically competitive than the former.

The isomer $CH_2CHCHCH$ **5** has four isomeric forms, **5a** (−96.9), **5b** (−94.0), **5c** (−94.2), and **5d** (−96.3), which can easily convert to each other. For simplicity, the isomerization that occurs among **5a**, **5b**, **5c**, and **5d** is not highlighted in the PES. Starting from **5**, five conversion pathways can be distinguished: (i) C–H cleavage to form $\mathbf{P_5}$ (CH_2CHCCH+H) (−65.1); (ii) C–C bond fission to form $\mathbf{P_7}$ (C_2H_2+C_2H_3) (−60.6); (iii) a 2,3 H shift to form CH_2CH_2CCH **8** (−94.2), followed by dissociation to $\mathbf{P_5}$ (CH_2CHCCH+H); (iv) a 1,2 H-shift to form CH_2CHCCH_2 **9** (−108.5), followed by dissociation to $\mathbf{P_6}$(CH_2CCCH_2+H), and; (v) ring closure to form the four-membered ring isomer c–C_4H_5 **10** (−105.1). By comparison, we find that channels (iii) and (iv) are more complicated than the former two channels. This means that channels (iii) and (iv) make only minor contributions to final fragmenta-

Table 1 Total (a.u.) and relative (kcal mol^{-1}; in parentheses) energies of the reactants, products, isomers and transition states for the CH +CH_3CCH reaction

Species	G3B3		Species	G3B3	
R (CH+CH_3CCH)	−155.0181405	(0.0)	TS1a/2	−155.0634426	(−28.4)
P_1 (CH_2CCH+CH_2)	−155.0188213	(−0.4)	TS1a/3	−155.0609201	(−26.8)
P_2 (CHCHCCH+H_2)	−155.107419	(−56.0)	TS1a/4	−155.0547313	(−23.0)
P_3 (CH_3−cCCCH+H)	−155.0631542	(−28.2)	TS1a/5a	−155.0526890	(−21.7)
P_4 (c−C_2H_3+CH_3)	−155.0692969	(−32.1)	TS1a/P_2	−155.0077792	(6.5)
P_5 (CH_2CHCCH+H)	−155.1218725	(−65.1)	TS1b/4	−155.0516006	(−21.0)
P_6 (CH_2CCCH_2+H)	−155.1103292	(−57.8)	TS1b/5b	−155.0542108	(−22.6)
P_7 (C_2H_2+C_2H_3)	−155.1138091	(−60.0)	TS2/6	−155.0470739	(−18.2)
P_8 (c−C_4H_4+H)	−155.0663693	(−30.3)	TS2/7	−155.0452505	(−17.0)
1a	−155.0655185	(−29.7)	TS3/8	−155.1152015	(−60.9)
1b	−155.0701953	(−32.7)	TS3/9	−155.0790935	(−38.2)
2	−155.1436700	(−78.8)	TS4/9	−155.1063828	(−55.4)
3	−155.1900752	(−107.9)	TS5a/5b	−155.1670148	(−93.4)
4	−155.1946474	(−110.8)	TS5a/5d	−155.1723985	(−96.8)
5a	−155.1725975	(−96.9)	TS5a/P_5	−155.1119040	(−58.8)
5b	−155.1679843	(−94.0)	TS5b/5c	−155.1616501	(−90.1)
5c	−155.1682111	(−94.2)	TS5b/8	−155.0983955	(−50.4)
5d	−155.1716076	(−96.3)	TS5b/9	−155.0961967	(−49.0)
6	−155.1260054	(−67.7)	TS5b/10	−155.1228339	(−65.7)
7	−155.1300564	(−70.2)	TS5b/P_5	−155.1044528	(−54.2)
8	−155.1683320	(−94.2)	TS5c/9	−155.1015868	(−52.4)
9	−155.1910534	(−108.5)	TS5c/P_7	−155.1053905	(−54.8)
10	−155.1856358	(−105.1)	TS5d/P_7	−155.1053931	(−54.8)
11	−155.0191142	(−0.6)	TS6/P_3	−155.0483644	(−19.0)
TS8/P_5	−155.1129354	(−59.5)	TS6/P_4	−155.0546771	(−22.9)
TS9/P_6	−155.1033057	(−53.4)	TS7/P_3	−155.0529547	(−21.8)
TS11/P_1	−154.9865006	(19.9)	TS8/11	−154.9894708	(18.0)

tion. Moreover, **10** would rather back-convert to **5b** than form **P_8** (c–C_4H_4+H).

On the other hand, the most important pathways from **1b** are those shown in Scheme 2. From Scheme 2, we can see that starting from CH_3CCHCH **1b** (32.7), two pathways can be identified: (i) a 1,2 H shift to form CH_3CCCH_2 **4** (−110.8), or (ii) a 2,3 H shift to form CH_2CHCHCH **5** (**5a**, **5b**, **5c**, **5d**) (−96.9, −94.0, −94.2, −96.3). The pathways of **4** and **5** have been discussed previously.

Reaction mechanism

In the preceding sections, we have identified eight important pathways for the CH+CH_3CCH reaction (paths **1**–**8**). By comparison, we find that paths **1**, **2**, **3**, and **6** are relatively simple, whereas the remaining paths are more complicated. For example, only one barrier needs to be surmounted in paths **1**, **2**, **3**, and **6**, which are 1.3 (**1a→2**) kcal mol^{-1} in path **1**, 2.9 (**1a→3**) kcal mol^{-1} in path **2**, 6.7 (**1a→4**) kcal mol^{-1} in path **3**, and 11.7 (**1b→4**) kcal mol^{-1} in path **6**, whereas two barriers must be negotiated in the other four paths, which are 8.0 (**1a→5a**) and 38.1 (**5a→P_5**) or 39.4 (**5b→P_5**) kcal mol^{-1} in path **4**, 8.0 (**1a→5a**) and 39.4 (**5c→P_6**) or 36.3 (**5d→P_6**) kcal mol^{-1} in path **5**, 10.1 (**1b→5b**) and 38.1 (**5a→P_5**) or 39.4 (**5b→P_5**) kcal mol^{-1} in path **7**, and 10.1 (**1b→5b**) and 39.4 (**5c→P_6**) or 36.3 (**5d→P_6**) kcal mol^{-1} in path **8**. Therefore, paths **4**, **5**, **7**, and **8** cannot compete with paths **1**, **2**, **3**, and **6**. It is difficult to judge the relative contributions of paths **1**, **2**, **3** and **6** because the barriers associated with these four paths are very similar. Thus, we can only tentatively predict that these four channels make comparable contributions to the title reaction.

We predict that the four dissociation products **P_3** (CH_3–cCCCH+H), **P_5** (CH_2CHCCH+H), **P_6** (CH_2CCCH_2+H) and **P_7** (C_2H_2+C_2H_3) may be observed, as reflected in the final product distributions. **P_3**, **P_5**, and **P_6** should be the most

Scheme 1 The most relevant pathways from 1a

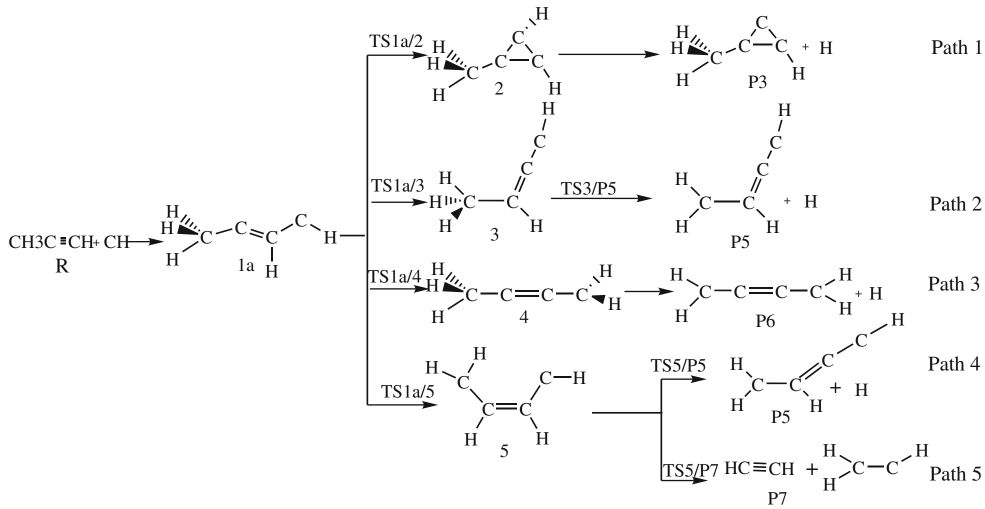

favorable products, all with comparable yields, whereas **P$_7$** should be the least competitive product.

Comparison with experiment

It is worth comparing our calculated results with previous experimental findings. In Goulay et al.'s experiment, the products and branching ratios were found be cyclic isomer + H (30%), vinylacetylene + H (37%), and 1,2,3-butatriene + H (33%) [26]. This is in excellent agreement with our theoretical result that **P$_3$** (CH_3–cCCCH + H), **P$_5$** (CH_2CHCCH+H), and **P$_6$** (CH_2CCCH_2+H) should be the most feasible products with comparable yields. Furthermore, based on our calculations, all of the isomers and transition states involved in the most feasible pathways lie below the reactant in energy, and the title reaction is expected to proceed rapidly, which is consistent with the large experimentally measured rate constants, i.e. $k = (4.03 \sim 4.56) \times 10^{-10} cm^3 molecule^{-1} s^{-1}$ (over the temperature range (15–295K)), as reported by Daugey et al. [21], and $k(300K) = (3.4 \pm 0.6) \times 10^{-10} cm^3 molecule^{-1} s^{-1}$, as reported by Loison et al. [25]. However, great discrepancies are found for the product distributions. Both Daugey et al. [21] and Loison et al. [25] suggested that the product is almost exclusively CH_2CCCH_2+H. However, our results show that **P$_5$** (CH_2CHCCH+H) and **P$_3$** (CH_3–cCCCH+H), which were competely ignored by Daugey et al. and Loison et al., may contribute to the final products to the same extent as **P$_6$** (CH_2CCCH_2+H). In view of these discrepancies, further investigations of the title reaction, especially the distribution of products, are highly desirable.

Conclusions

The reaction of CH with CH_3CCH was theoretically studied at the B3LYP/6-311G(d,p) and G3B3 (single-point) levels. Our results show that four kinds of dissociation products may be observed. Among these products, **P$_3$** (CH_3–cCCCH+H), **P$_5$** (CH_2CHCCH+H), and **P$_6$** (CH_2CCCH_2+H) may be the most feasible products, and are produced in comparable yields, whereas **P$_7$** (C_2H_2+C_2H_3) may be easily the least competitive product. The present paper is the first theoretical study of the title reaction. We hope that our calculated results may shed some light on the mechanism of the CH+CH_3CCH reaction.

Scheme 2 The most relevant pathways from 1b

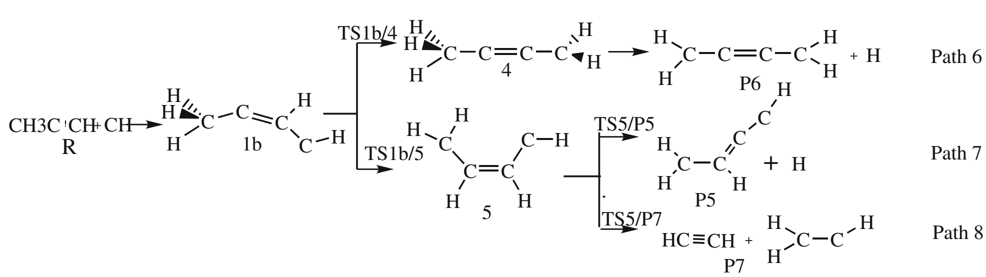

Acknowledgments This work is supported by the National Natural Science Foundation of China (nos. 20773048, 21073075)

References

1. Sanders WA, Lin MC (1986) In chemical kinetic of small organic radical, vol III. CRC, Boca Raton
2. Miller JA, Kee RJ, Westbrook CK (1990) Annu Rev Phys Chem 41:345–387
3. Lindqvist M, Sandqvist A, Winnberg A, Johansson L, Nyman LA (1995) Astron Astrophys Suppl Ser 113:257–263
4. Canosa A, Sims IR, Travers D, Smith IWM, Rowe BR (1997) Astron Astrophys 323:644–651
5. Amin MY, El-Nawawy MS (1996) Earth Moon Planet 75:25–39
6. Brownsword RA, Sims IR, Smith IWM (1997) Astrophys J 485:195–201
7. Herzberg G, Johns JWC (1969) Astrophys J 58:399–406
8. Bernath PF (1987) J Chem Phys 86:4838–4842
9. Zachwieja M (1995) J Mol Spectrosc 170:285–289
10. Kalemos A, Mavridis A, Metropoulos A (1999) J Chem Phys 111:9536–9548
11. Hirata S, Yanai T, Jong WA, Nakajima T, Hirao K (2004) J Chem Phys 120:3297–3310
12. Vázquez GJ, Amero JM, Liebermann HP, Buenker RJ, Lefebvre-Brion H (2007) J Chem Phys 126:164302–164315
13. Ikejiri K, Ohoyama H, Nagamachi Y, Kasai T (2005) Chem Phys Lett 401:465–469
14. Manaa MR, Yarkony DR (1991) J Chem Phys 95:1808–1817
15. Seideman T, Walch SP (1994) J Chem Phys 101:3656–3662
16. Seideman T (1994) J Chem Phys 101:3662–3671
17. Berman MR, Tsuchiya T, Gregušová A, Perera SA, Bartlett RJ (2007) J Phys Chem A 111:6894–6899
18. Bergeat A, Calvo T, Dorthe G, Loison JC (1999) J Phys Chem A 103:6360–6365
19. Jursic BS (1998) J Phys Chem A 102:9255–9260
20. Fleurat-Lessard P, Rayez JC, Bergeat A, Loison AC (2002) Chem Phys 279:87–99
21. Daugey N, Caubet P, Retail B, Costes M, Bergeat A, Dorthe G (2005) Phys Chem Chem Phys 7:2921–2927
22. Loison JC, Bergeat A, Caralp F, Hannachi Y (2006) J Phys Chem A 110:13500–13506
23. Mckee K, Blitz MA, Hughes KJ, Pilliing MJ, Qian HB, Taylor A, Seakins PW (2003) J Phys Chem A 107:5710–5716
24. Galland N, Caralp F, Hannachi Y, Bergeat A, Loison JC (2003) J Phys Chem A 107:5419–5426
25. Loison JC, Bergeat A (2009) Phys Chem Chem Phys 11:655–664
26. Goulay F, Trevitt AJ, Meloni G, Selby TM, Osborn DL, Taatjes CA, Vereecken L, Leone SR (2009) J Am Chem Soc 131:993–005
27. Frisch MJ, Trucks GW, Schlegel HB et al (2004) Gaussian 03, revision D.02. Gaussian Inc., Wallingford